

Terahertz emission from magnetic thin film and patterned heterostructures

Sergi Lendinez^a, Yi Li^b, Weipeng Wu^a, Mojtaba Taghipour Kaffash^a, Qi Zhang^c, Wei Zhang^{b,d}, John. E. Pearson^b, Ralu Divan^e, Richard D. Schaller^{e,f}, Axel Hoffmann^b, Haidan Wen^c, and Matthias B. Jungfleisch^a

^aDepartment of Physics and Astronomy, University of Delaware, Newark, Delaware 19716, USA

^bMaterials Science Division, Argonne National Laboratory, Argonne, Illinois 60439, USA

^cAdvanced Photon Source, Argonne National Laboratory, Argonne, Illinois 60439, USA

^dDepartment of Physics, Oakland University, Rochester, Michigan 48309, USA

^eCenter for Nanoscale Materials, Argonne National Laboratory, Argonne, Illinois 60439, USA

^fDepartment of Chemistry, Northwestern University, Evanston, Illinois 60208, USA

ABSTRACT

In recent years terahertz (THz) technology has been an emerging research field with a broad range of applications. THz radiation falls between the infrared and microwave radiation in the electromagnetic spectrum. Most THz sources to date are not related to the spin degree of freedom; however, recent research efforts in spintronics and ferromagnetism demonstrated that the electron spin offers completely new opportunities for the generation of ultrafast photocurrents. For instance, magnetic heterostructures are very easy to pattern and potentially allow to tailor THz emission characteristics by design. Here, we demonstrate that an ultrafast spin-current pulse driven by a femtosecond laser pulse can create THz transients in microstructured magnetic heterostructures due to the inverse spin Hall effect. We compare the THz electric field and the THz spectrum of a control CoFeB/Pt film with microstructured CoFeB/Pt wires as well as microstructured CoFeB/MgO wires patterned on an extended Pt film. We find that the THz electric field amplitude is proportional to the coverage of the CoFeB/Pt heterostructure on top of the MgO substrate. Furthermore, we analyze the magnetization direction dependence of the THz transients with respect to the easy axis of the ferromagnetic wire. The presented results are the first steps towards shaping and controlling the THz properties by microstructuring of spintronics-based THz emitters.

Keywords: Terahertz spintronics, spin Hall effect, magnetic microstructure, spintronics

1. INTRODUCTION

Over the past decade, terahertz (THz) technology has been an emerging research field with great potential for a vast range of applications. THz radiation is defined as electromagnetic radiation that falls between infrared and microwave radiation. It can be used for a variety of material characterization such as advanced diagnostics, medical imaging, security systems, and atmospheric studies. Standard THz sources such as semiconductor-based photoconductive antennas or nonlinear crystals rely on the electron's charge. Very recently, however, it was realized that it is possible to exploit the electron's spin for the generation of THz radiation paving the way for "THz spintronics".¹ These spintronics devices allow for the development of novel, low-cost, efficient, broadband THz emitters, which are easily customizable by a manipulation of the spin degree of freedom via, e.g., the bias magnetic field.

Kampfrath et al. demonstrated that a laser pulse can drive a spin current from an iron thin film into a non-magnetic capping layer (Ru and Au),² where the spin current is converted into a charge current by the

Further author information: (Send correspondence to M.B.J.)

M.B.J.: E-mail: mbj@udel.edu, Telephone: 1 302 831 8787

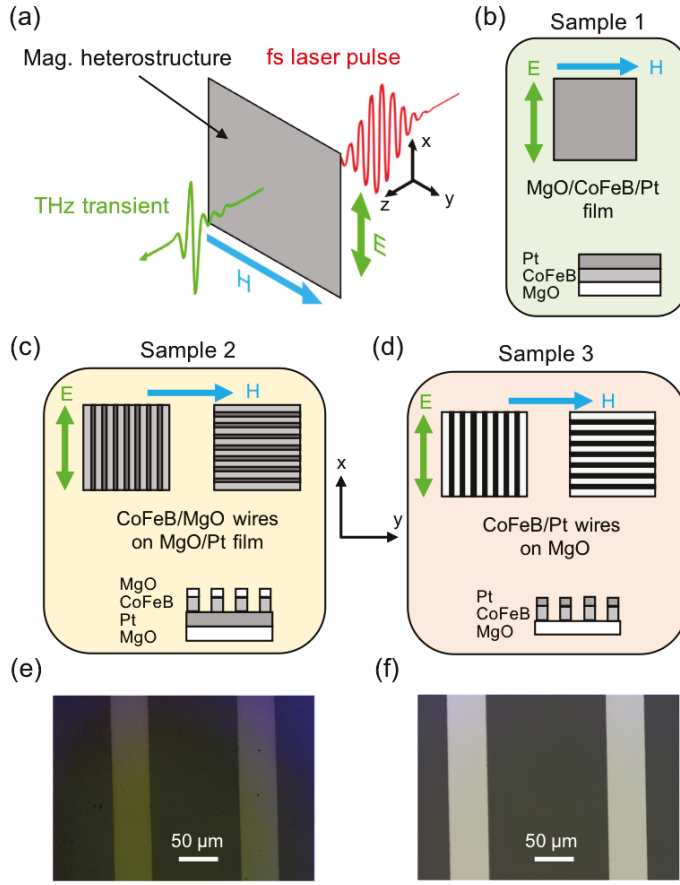


Figure 1. (a) Schematic of the experimental setup and sketch of THz emission from magnetic heterostructures. Magnetic field H (blue) is applied horizontally, the direction of detected THz electric field E (green) is vertical. (b) - (c) Three different types of magnetic heterostructures are studied using the setup shown in (a). (b) Control sample consisting of an extended CoFeB(3)/Pt(3) film grown on an MgO substrate, sample 1. (b) Extended Pt film with a thickness of 3 nm is grown on the MgO substrate. CoFeB(3)/MgO(3) wires with a width of 49 μm and a separation of 115 μm are defined on top of the Pt film, sample 2. An optical microscope image is shown in (e). (d) CoFeB(3)/Pt(3) wires are patterned on the MgO substrate, sample 3. Wire width: 49 μm , separation: 154 μm . An optical microscope image is shown in (f).

inverse spin Hall effect.^{3,4} More recently, it was shown that by using this type of magnetic heterostructure it is possible to fabricate ultrabroadband THz emitters⁵ that can provide large peak fields of up to 300 kV/cm.⁶ These emitters even outperform standard laser-driven emitters such as nonlinear crystals in terms of bandwidth, terahertz field amplitude, flexibility, scalability and cost.⁵ Furthermore, it was shown that magnetic insulators (yttrium iron garnet) can be used as THz sources^{7,8} and the effect of the magnetization alignment on the THz generation process was discussed.⁹ Besides the inverse spin Hall effect, it was shown that other effects based on spin-orbit coupling can be used for efficient THz emission. In particular, it was shown that femtosecond spin-current pulses can generate terahertz transients at Rashba interfaces between nonmagnetic materials, i.e., Ag/Bi.^{10,11} First attempts to use patterned magnetic heterostructures for the generation of THz transients was presented by Yang et al.¹² However, the microstructured stripes were much narrower than the wavelength of the THz radiation.

One major advantage of spintronic-based THz emitters is the prospect of effectively manipulating the THz emission characteristics by engineering the source structure. Here, we demonstrate that an ultrafast spin-current pulse driven by a femtosecond laser pulse can create THz transients in microstructured magnetic heterostructures made of CoFeB and Pt. We compare the THz electric field and the THz spectrum of a control CoFeB/Pt film

with microstructured CoFeB/Pt wires as well as microstructured CoFeB/MgO wires patterned on an extended Pt film. We find that the THz electric field amplitude is proportional to the area coverage of the CoFeB/Pt heterostructure on top of the MgO substrate. Furthermore, we analyze the magnetization direction dependence of the THz transients with respect to the easy axis of the ferromagnetic wire. This finding is compared to results obtained from micromagnetic simulations.

2. EXPERIMENTAL DETAILS

We fabricated the samples using dc magnetron sputtering in an Ar atmosphere at 5 mTorr and 30 sccm gas flow (base pressure $< 1 \times 10^{-7}$ Torr) on double-side-polished MgO substrates with a (100) orientation. The following sputtering parameters have been used: CoFeB, sputtering rate 0.18 Å/s at 9 W; Pt sputtering rate 0.9 Å/s at 10 W; MgO sputtering rate 0.2 Å/s at 60 W; Ti sputtering rate 0.3 Å/s at 20 W. Three different types of samples were fabricated (thickness in parentheses in nanometers): (A) Sample 1: Extended Ti(2)/CoFeB(3)/Pt(3) film grown on a MgO substrate as shown in Fig. 1(b); (B) Sample 2: Extended Pt(3) film grown on a MgO substrate. In a second lithography process CoFeB(3)/MgO(3) wires with a width of 49 μ m and a separation of 115 μ m were defined on top of the Pt film as shown in Fig. 1(c). An optical micrograph of the sample is shown in Fig. 1(e); (C) Sample 3: 49 μ m wide wires (separation 154 μ m) made of Ti(2)/CoFeB(3)/Pt(3) were grown on a MgO substrate as shown in Fig. 1(d). An optical micrograph of the sample is shown in Fig. 1(f). The wires of samples 2 and 3 were patterned using optical lithography and lift-off. Please note that the additional MgO layer for the second sample is a capping layer that prevents oxidation of the CoFeB layer. Ti was used as a seed layer for samples 1 and 3 (not shown in the schematic).

The experimental setup and the corresponding measurement orientation is shown in Fig. 1(a). The incident laser pulse is aligned perpendicular to the sample plane and faces the MgO substrate. The optical pump is derived from a 2 kHz Ti:sapphire regenerative amplifier with 800 nm in wavelength and 35 fs pulse width. The laser power at the sample is 340 mW and the beam diameter is 3 mm (full width at half maximum). The THz electric field generated by the spintronics-based emitters is measured after a pair of wire-grid polarizer using electro-optical sampling.¹³ The wire-grid polarizer is oriented so that a maximum THz field was detected from the control sample consisting of an extended CoFeB/Pt film deposited on a MgO substrate [see Fig. 1(b)]. For the electro-optical sampling, a 300 μ m thick (110) ZnTe crystal is used. A bias magnetic field of constant magnitude is applied in a fixed direction (in the sample plane) to align the CoFeB magnetization \vec{m} . For the control sample only one measurement configuration is used as shown in Fig. 1(b): the magnetic field is applied in the sample plane perpendicular to the incident laser pulse. In case of the microstructured samples, the ferromagnetic wires are aligned either perpendicular (x -direction) or parallel (y -direction) to the bias magnetic field (y -direction).

3. RESULTS AND DISCUSSION

Figure 2(a) shows terahertz signal waveforms measured from photoexcitation of the extended film control sample and the microstructured samples; the corresponding Fourier-transformed signals are shown in Fig. 2(b). In the experiments, an ultrafast spin current in the CoFeB layer is generated by the absorption of the femtosecond laser pulse that leads to a nonequilibrium spin distribution in CoFeB. Due to the imbalance of majority-spin and minority-spin electrons, a spin-polarized electron current \vec{j}_s diffuses from the CoFeB into the Pt layer, where it is converted to a charge current bunch \vec{j}_c by the inverse spin Hall effect.²

$$\vec{j}_c \propto \gamma \vec{j}_s \times \vec{m}, \quad (1)$$

where \vec{m} is the sample magnetization and γ is the spin Hall angle, which is a material specific parameter. An interesting feature of the time traces shown in Fig. 2(a) is that the sample consisting of an extended CoFeB/Pt control film (sample 1) and the CoFeB/Pt wires (sample 3) have the same phase, while the signal observed from the CoFeB wires patterned on top of an extended Pt film (sample 2) is 180° phase shifted. The reason for that is that a spin current with a spin-polarization vector of opposite sign is injected into the Pt layer due to the inverted stacking order. This leads in turn to an inversion of the signal (see also Fig. 1 for a schematic of the sample stacking).

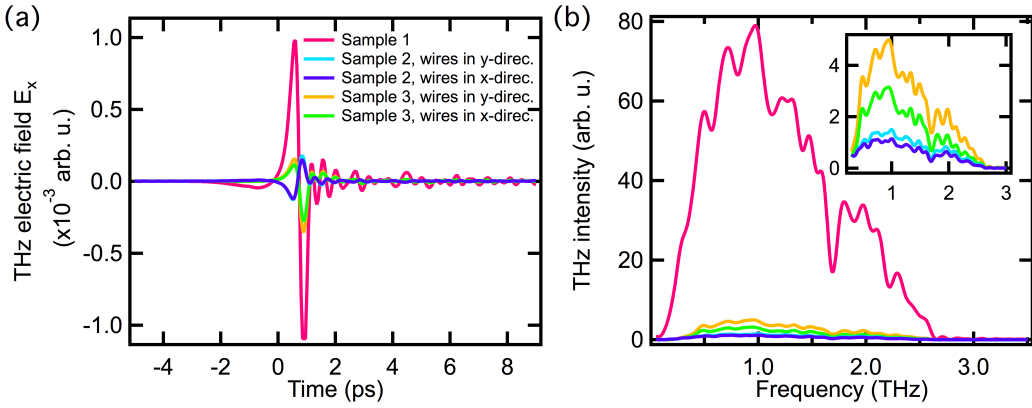


Figure 2. (a) Comparison of THz electric field E_x generated by the studied magnetic heterostructures. The phase shift of the CoFeB/MgO wires grown on the extended Pt film is caused by the reverse stacking order as illustrated in Fig. 1. (b) Corresponding Fourier transform of the time-resolved measurements shown in (a). The inset shows the THz intensity of the microstructured magnetic heterostructures on a magnified scale.

As is obvious from Fig. 2(a), the THz electric field of the control sample is significantly larger than that of any of the microstructures. This can be understood by the fact that in the case of the microstructured samples the ferromagnetic layer covers only a fraction of the substrate area and is therefore contributing less to the THz signal output. Please note that the magnetic CoFeB layer is necessary for the THz generation process as it serves as a spin-current source. On the other hand, the Pt layer is required for the spin-to-charge current conversion process due to the inverse spin Hall effect. We demonstrated in an earlier work¹⁰ that a layer of a spin-to-charge converter material alone does not generate any THz radiation, while a bare CoFeB layer does produce a small, yet detectable, THz signal. There are three possible sources that could contribute to the signal from a bare CoFeB layer: (i) Inverse Rashba Edelstein effect that occurs at surfaces when space inversion symmetry is broken. (ii) CoFeB itself may show a nonzero spin-Hall angle resulting in spin-charge conversion in the CoFeB layer.¹⁴⁻¹⁶ (iii) Ultrafast demagnetization processes in the CoFeB layer may lead to a THz radiation.¹

In the following we relate the material coverage to the magnitude of the generated THz electric field. The laser beam with a polarization in x -direction is aligned perpendicular to the sample plane and the wires are aligned either parallel (x -direction) or perpendicular (y -direction) to the laser polarization. The beam diameter is 3 mm, which implies that approximately 14 - 15 wires are excited at a time. In the microstructured samples, CoFeB covers approximately 24% of the illuminated area. In Tab. 1 we compare the magnitude of the THz electric field (defined as the difference between maximum and minimum), as well as the magnitudes of the various samples normalized to the reference sample (sample 1, CoFeB/Pt film). First we discuss the results of sample 3 (CoFeB/Pt wires on MgO) [Fig. 1(d)]. When the bias magnetic field is aligned parallel to the long axis of the wires (y -direction) the magnitude of the THz field is about 24.6% of that of the reference CoFeB/Pt film (sample 1). This agrees well with the fact that in case of the microstructured sample only 24% of the illuminated area is “active”. Rotating the sample 90° results in a slightly smaller signal: the magnitude is about 19%. In contrast, the sample with CoFeB wires patterned on top of an extended Pt film (sample 2) shows a magnitude that is only 14.8% of the reference sample (sample 1) when the wires are aligned parallel to the bias magnetic field (y -direction), and 13% when the wires are aligned perpendicular to the field (x -direction). From a comparison of sample 2 and sample 3, it seems likely that the lower THz electric field magnitude of sample 2 stems from the fact that the Pt layer reflects a non-negligible amount of the optical pump pulse before exciting the CoFeB layer. Thus, a smaller spin-current is excited in the CoFeB layer.

Another remarkable feature of the results shown in Fig. 2 is the dependence of the signal magnitude on the relative orientation of the wires with respect to the bias magnetic field. Independent of whether the wires are patterned on the Pt film (sample 2), or both CoFeB and Pt are patterned into wires (sample 3), we find a

Sample	THz field magnitude (arb. u.)	Normalized magnitude (%)
Sample 1	2.08×10^{-3}	100
Sample 2, wires in y -direction	3.07×10^{-4}	14.8
Sample 2, wires in x -direction	2.71×10^{-4}	13.0
Sample 3, wires in y -direction	5.11×10^{-4}	24.6
Sample 3, wires in x -direction	3.93×10^{-4}	19.0

Table 1. Comparison of different samples and measurements configurations. Sample 1: reference sample consisting of an extended CoFeB/Pt film, Fig. 1(b). Sample 2: CoFeB/MgO wires on Pt film, Fig. 1(c). Sample 3: CoFeB/Pt wires, Fig. 1(d). x -direction: perpendicular to bias magnetic field, y -direction: parallel to bias magnetic field.

slightly smaller magnitude when the wires are oriented perpendicular to the magnetic field (x -direction). This is in contrast to the recent results reported by Yang et al.¹² where a larger signal was observed when the field was applied perpendicular to the stripes. They concluded that the transient transverse charge current flows perpendicular to the stripes when field is applied along the long axis of the wire, which will lead to a charge accumulation at the stripe edges inhibiting the initial transient charge current. Thus, a smaller THz signal was observed. However, the wires in our experiment are approximately 10 times wider and the separation between the wires approximately 30 times bigger than in the work by Yang et al. Therefore, the electric field due to the charge build up is significantly lower and thus does not inhibit the transient charge current.

In the following we qualitatively explain the smaller THz magnitude observed when the wires are aligned in the x -direction (perpendicular to the magnetic field). One possible reason for this finding is that the bias magnetic field is insufficiently large to overcome the shape anisotropy and thus the magnetization in the edge regions points in the x -direction, not contributing to the x -component of the THz electric field. To confirm this scenario we performed micromagnetic simulations using MuMax3.¹⁷ The actual sample dimensions are too large to be simulated. Therefore, a smaller wire width of $3 \mu\text{m}$ and a length of $12 \mu\text{m}$ was chosen. The results of the simulations are shown in Fig. 3 as color-coded images of the x -component of the magnetization for $H = 600 \text{ Oe}$. The left figures show a wire oriented perpendicular; the right figures show a wire oriented parallel to the bias magnetic field. As is obvious from the figure, 600 Oe is not large enough to compensate for shape anisotropy when the wire is aligned in the x -direction. As a result, the magnetization in the edge regions points perpendicular to the applied field. Our measurement setup is insensitive to a spin-to-charge conversion of a spin current originating from these areas of the sample, and thus an overall smaller signal is detected. This area is much smaller for a wire orientation in y -direction as shown on the right in Fig. 3.

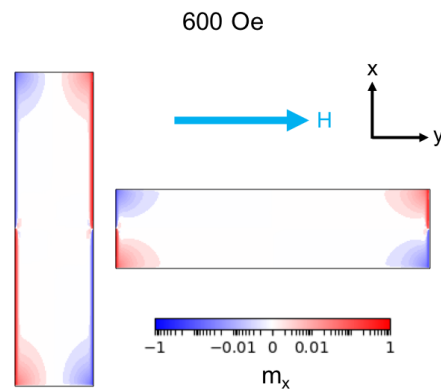


Figure 3. Results of micromagnetic simulations. The x -component of the magnetization is shown in a 2D plot as a color-coded image for a bias magnetic field of $H = 600 \text{ Oe}$. Two configurations are shown: Left - wire axis parallel to the bias magnetic field H , y -direction; right - wire axis perpendicular to the bias magnetic field H , x -direction. The simulated wire width is $3 \mu\text{m}$, length $12 \mu\text{m}$, thickness 9 nm . The cell size is 5 nm .

4. CONCLUSION

We showed that an ultrafast spin-current pulse driven by a femtosecond laser pulse can create THz transients due to the inverse spin Hall effect in microstructured magnetic heterostructures made of CoFeB and Pt. We found that the strength of the THz electric field is proportional to the area coverage of the CoFeB/Pt heterostructure on top of the MgO substrate as the laser beam illuminates the entire sample area. Furthermore, we analyzed the magnetization direction dependence of the THz transients with respect to the easy axis of the ferromagnetic wire. By comparing these results with micromagnetic simulations we found that a small portion of the moments at the edges of the micro-wires lie in the easy axis independent of the applied magnetic field, which reduces the overall spin current that contributes to the THz signal. Thus, the magnitude of the THz electric field is slightly smaller when the bias magnetic field is applied perpendicular to the long axis (easy axis) of the wires. The presented results are the first steps towards shaping and controlling the THz properties by microstructuring of spintronics-based THz emitters.

ACKNOWLEDGMENTS

This work was supported by the National Science Foundation under Grant No. 1833000. Thin film deposition was performed at Argonne and supported by the U.S. Department of Energy, Office of Science, Materials Science and Engineering Division. Use of the Center for Nanoscale Materials, an Office of Science user facility, was supported by the U.S. Department of Energy, Office of Science, Office of Basic Energy Sciences, under Contract No. DE-AC02-06CH11357.

REFERENCES

- [1] Walowski, J. and Münzenberg, M., “Perspective: Ultrafast magnetism and THz spintronics,” *Journal of Applied Physics* **120**(14), 140901 (2016).
- [2] Kampfrath, T., Battiatto, M., Maldonado, P., Eilers, G., Nötzold, J., Mährlein, S., Zbarsky, V., Freimuth, F., Mokrousov, Y., Blügel, S., Wolf, M., Radu, I., Oppeneer, P. M., and Münzenberg, M., “Terahertz spin current pulses controlled by magnetic heterostructures,” *Nature Nanotechnology* **8**(4), 256–260 (2013).
- [3] Dyakonov, M. I. and Perel, V. I., “Possibility of Orienting Electron Spins with Current,” *Sov. JETP Lett.* **13**, 467 (1971).
- [4] Hoffmann, A., “Spin Hall Effects in Metals,” *IEEE Transactions on Magnetics* **49**(10), 5172–5193 (2013).
- [5] Seifert, T., Jaiswal, S., Martens, U., Hannegan, J., Braun, L., Maldonado, P., Freimuth, F., Kronenberg, A., Henrizi, J., Radu, I., Beaurepaire, E., Mokrousov, Y., Oppeneer, P. M., Jourdan, M., Jakob, G., Turchinovich, D., Hayden, L. M., Wolf, M., Münzenberg, M., Kläui, M., and Kampfrath, T., “Efficient metallic spintronic emitters of ultrabroadband terahertz radiation,” *Nature Photonics* **10**(7), 483–488 (2016).
- [6] Seifert, T., Jaiswal, S., Sajadi, M., Jakob, G., Winnerl, S., Wolf, M., Kläui, M., and Kampfrath, T., “Ultrabroadband single-cycle terahertz pulses with peak fields of 300 kV cm⁻¹ from a metallic spintronic emitter,” *Applied Physics Letters* **110**(25), 252402 (2017).
- [7] Seifert, T. S., Jaiswal, S., Barker, J., Weber, S. T., Razdolski, I., Cramer, J., Gueckstock, O., Maehrlein, S. F., Nadvornik, L., Watanabe, S., Ciccarelli, C., Melnikov, A., Jakob, G., Münzenberg, M., Goennenwein, S. T. B., Woltersdorf, G., Rethfeld, B., Brouwer, P. W., Wolf, M., Kläui, M., and Kampfrath, T., “Femtosecond formation dynamics of the spin Seebeck effect revealed by terahertz spectroscopy,” *Nature Communications* **9**, 363001 (July 2018).
- [8] Cramer, J., Seifert, T., Kronenberg, A., Fuhrmann, F., Jakob, G., Jourdan, M., Kampfrath, T., and Kläui, M., “Complex Terahertz and Direct Current Inverse Spin Hall Effect in YIG/Cu_{1-x}Ir_x Bilayers Across a Wide Concentration Range,” *Nano Letters* **18**(2), 1064–1069 (2018).
- [9] Schneider, R., Fix, M., Heming, R., Michaelis De Vasconcellos, S., Albrecht, M., and Bratschitsch, R., “Magnetic-Field-Dependent THz Emission of Spintronic TbFe/Pt Layers,” *ACS Photonics* **5**, 3936–3942 (Oct. 2018).
- [10] Jungfleisch, M. B., Zhang, Q., Zhang, W., Pearson, J. E., Schaller, R. D., Wen, H., and Hoffmann, A., “Control of Terahertz Emission by Ultrafast Spin-Charge Current Conversion at Rashba Interfaces,” *Physical Review Letters* **120**, 207207 (May 2018).

- [11] Zhou, C., Liu, Y. P., Wang, Z., Ma, S. J., Jia, M. W., Wu, R. Q., Zhou, L., Zhang, W., Liu, M. K., Wu, Y. Z., and Qi, J., "Broadband Terahertz Generation via the Interface Inverse Rashba-Edelstein Effect," *Physical Review Letters* **121**, 086801 (Aug. 2018).
- [12] Yang, D., Liang, J., Zhou, C., Sun, L., Zheng, R., Luo, S., Wu, Y., and Qi, J., "Powerful and Tunable THz Emitters Based on the Fe/Pt Magnetic Heterostructure," *Advanced Optical Materials* **4**(12), 1944–1949 (2016).
- [13] Peiponen, K.-E., Zeitler, A., and Kuwata-Gonokami, M., [*Terahertz Spectroscopy and Imaging*], Springer Series in Optical Sciences, Springer, Berlin (2013).
- [14] Azevedo, A., Santos, O. A., Cunha, R. O., Rodríguez-Suárez, R., and Rezende, S. M., "Addition and subtraction of spin pumping voltages in magnetic hybrid structures," *Applied Physics Letters* **104**, 152408 (Apr. 2014).
- [15] Tsukahara, A., Ando, Y., Kitamura, Y., Emoto, H., Shikoh, E., Delmo, M. P., Shinjo, T., and Shiraishi, M., "Self-induced inverse spin Hall effect in permalloy at room temperature," *Physical Review B* **89**, 235317 (June 2014).
- [16] Weiler, M., Shaw, J. M., Nembach, H. T., and Silva, T. J., "Detection of the DC Inverse Spin Hall Effect Due to Spin Pumping in a Novel Meander-Stripline Geometry," *IEEE Magnetics Letters* **5**, 1–4 (2014).
- [17] Vansteenkiste, A., Leliaert, J., Dvornik, M., Helsen, M., Garcia-Sanchez, F., and Van Waeyenberge, B., "The design and verification of MuMax3," *AIP Advances* **4**, 107133 (Oct. 2014).